RESEARCH ARTICLE

Proteome analysis of wheat leaf rust fungus, *Puccinia triticina*, infection structures enriched for haustoria

Xiao Song[1], Christof Rampitsch[2], Bahram Soltani[1], Wayne Mauthe[2], Rob Linning[1], Travis Banks[2], Brent McCallum[2] and Guus Bakkeren[1]

[1] Agriculture & Agri-Food Canada, Pacific Agri-Food Research Centre, Summerland, BC, Canada
[2] Agriculture & Agri-Food Canada, Cereal Research Centre, Winnipeg, MB, Canada

Received: January 8, 2010
Revised: November 22, 2010
Accepted: December 5, 2010

Puccinia triticina (*Pt*) is a representative of several cereal-infecting rust fungal pathogens of major economic importance world wide. Upon entry through leaf stomata, these fungi establish intracellular haustoria, crucial feeding structures. We report the first proteome of infection structures from parasitized wheat leaves, enriched for haustoria through filtration and sucrose density centrifugation. 2-D PAGE MS/MS and gel-based LC-MS (GeLC-MS) were used to separate proteins. Generated spectra were compared with a partial proteome predicted from a preliminary *Pt* genome and generated ESTs, to a comprehensive genome-predicted protein complement from the related wheat stem rust fungus, *Puccinia graminis* f. sp. *tritici* (*Pgt*) and to various plant resources. We identified over 260 fungal proteins, 16 of which matched peptides from *Pgt*. Based on bioinformatic analyses and/or the presence of a signal peptide, at least 50 proteins were predicted to be secreted. Among those, six have effector protein signatures, some are related and the respective genes of several seem to belong to clusters. Many ribosomal structural proteins, proteins involved in energy, general metabolism and transport were detected. Measuring gene expression over several life cycle stages of ten representative candidates using quantitative RT-PCR, all were shown to be strongly upregulated and four expressed solely upon infection.

Keywords:
Basidiomycete / Haustorium / Microbiology / *Puccinia recondita* / WLR

1 Introduction

Understanding the interaction of pathogens with their respective hosts on genetic, cell biological and biochemical levels is essential for designing novel strategies to combat disease. In agronomic settings, such knowledge is widely expected to lead to the accelerated discovery of novel sources of host resistance and the design of increased durable disease resistance in crop plants (e.g. [2]). Several model microbial-host pathosystems are being studied in depth but some of the major crop disease systems remain poorly understood. One of the most challenging pathosystems having major economical impact world-wide includes a group of related basidiomycete rust fungi infecting cereal crops. These pathogens belong to the genus *Puccinia* and genomic resources are being developed for *Puccinia graminis* f. sp. *tritici* (*Pgt*), causing wheat stem rust [3], *Puccinia triticina* Eriks. (*Pt*, formerly known as *Puccinia recondita* f. sp. *tritici*) causing wheat leaf or brown rust [4] and *Puccinia striiformis* f. sp. *tritici* (*Pt* [5]). Expressed sequence tag (EST) collections and a near-complete genome for *Pgt* became publicly available in 2007, and a partial genome for *Pt* in 2009 (http://www.broadinstitute.org/annotation/genome/puccinia_group.1/MultiHome.html). We have been focusing on *Pt* and contributed a large EST resource [6] which we have expanded. These genomic resources allowed us to embark on a proteomics-based search for proteins involved in the infection process.

Correspondence: Dr. Guus Bakkeren, Agriculture and Agri-Food Canada, Pacific Agri-Food Research Centre, 4200 Hwy 97, Summerland, BC, V0H 1Z0, Canada
E-mail: guus.bakkeren@agr.gc.ca
Fax: +1-250-494-0755

Abbreviations: BLAST, Basic Local Alignment Search Tool [1]; **GeLC-MS,** gel-based LC-MS; **NCBI,** National Centre for Biotechnology Information; ***Pgt,*** *Puccinia graminis* f. sp. *tritici* (wheat stem rust fungus); ***Pt,*** *Puccinia triticina* (wheat leaf rust fungus); **qRT-PCR,** quantitative RT-PCR

P. triticina has a complex life cycle which includes five different spore types and two hosts: wheat (*Triticum aestivum* L.) and meadow rue (*Thalictrum speciosissimum* L.). The latter species is the alternate host on which the fungus completes its sexual stage [4, 7, 8]. Sex is not essential and the infection of and spread on wheat through re-infection of urediniospores constitute the asexual cycle familiar to most and can lead to epidemics. Early processes in infection after urediniospores land on wheat leaf surfaces include attachment and the formation of a germ tube upon germination which searches for natural openings, the stomata. Once found, the tip of the germtube differentiates into an appressorium over the stomatal lips. Entry into the substomatal cavity is gained forcibly by turgor pressure upon which a haustorial mother cell is formed adjacent to a plant cell. Under favorable conditions, within 24 h, actual cell wall penetration takes place here and invagination of the host plasmalemma results in the first intimate contact. Thereafter, a microscopically visible haustorial interface surrounding the mature feeding structure is produced, likely made up of both fungal and host material [9]. This extra-haustorial matrix is critical in governing protein and metabolite traffic and establishing the feeding interaction [10–12].

Haustoria are thought to deliver, via secretion, a suite of proteins and metabolites aimed at suppressing host defense responses that may have been triggered by the fungus upon entering, and at reprogramming the host to treat the haustoria as nutrient sinks and divert nutrients to them. As such, secreted components can be defined as virulence factors or 'effectors' [2, 13]. In bacterial systems, effectors have been shown to be delivered into host cells through a type III secretion system (TTSS [14, 15]), but in fungi and oomycete pathogens the mechanism remains unknown [16, 17]. Certain effectors are recognized by the host 'surveillance system' of which the resistance or *R*-genes are a part and can trigger an immune response. Such effectors have been described by their genetic term as 'avirulence factors' (coded for by avirulence genes) since they render the pathogen avirulent on host cultivars harboring the cognate *R*-gene. It appears that such incompatible interactions, often leading to local programmed cell death through a hypersensitive response (necrosis), occur during or shortly after the haustorium is established [18, 19]. Our analysis of an initial set of *P. triticina* ESTs alluded to increased protein production and metabolism upon host infection [6] but also identified small *P. triticina* proteins whose homologs were identified as being specifically expressed in haustoria or infected leaves in other fungal biotrophs; some were predicted to be secreted [20–22].

Given the importance of the haustorium, we set out to obtain an initial inventory of the fungal proteins produced in this differentiated structure that could confirm earlier EST work and possibly reveal further clues about how it functions. We were also interested in the discovery of candidate small secreted proteins to investigate the feasibility of revealing the effector repertoire in enriched haustorial fractions. Due to the difficulty in isolating haustoria from infected plant leaves and generating protein information from these, only two studies have recently been published investigating a similarly pathosystem. Partial proteomes were reported from enriched haustoria from barley leaves infected with the biotrophic powdery mildew fungus, *Blumeria graminis* f. sp. *hordei* [23, 24]. In the present study, we have optimized protocols combining filtration and sucrose gradient density centrifugation to obtain enriched fractions of isolated haustoria from infected wheat leaf tissue.

We used two proteomic approaches for the analysis of haustorial-enriched proteins. We first employed a combination of 2-DE and LC-MS. Relatively few spots containing sufficient amounts of protein could be selected and therefore, secondly, we used a combination of SDS-PAGE and LC-MS (termed gel-based LC-MS (GeLC-MS) [25]), which combines the solubilization power of SDS with two dimensions of separation, the first based on protein M_r by electrophoresis and the second based on peptide hydrophobicity by reversed-phase HPLC. Tentative protein identification was achieved through homology matching of the predicted proteins from the partial *Pt* genome and the extensive EST collection, and predicted proteins from the related *Pgt* genome.

2 Materials and methods

2.1 Fungal and plant material

Wheat (*T. aestivum*) cultivar Thatcher (RL 6101), which is susceptible to *P. triticina* race 1 (designated BBBD [26]) was used in this study. Seedlings were grown in 10-cm pots maintained at 18–22°C in a leaf rust-free greenhouse with a photoperiod of approximately 12 h. Rust inoculations were performed on 10-day-old seedlings as described by Hu and Rijkenberg [19]. In short, urediniospores were mixed with light mineral oil (Soltrol 130 isoparaffin, Chevron Phillips Chemical, Borger, TX, USA) and sprayed onto the leaves using an air-powered sprayer. For mock inoculation, an equivalent volume of mineral oil was applied. After 30 min to allow the oil to evaporate, plants were moved to a dark dew chamber with nearly 100% relative humidity for 24 h to allow for optimal urediniospore germination and infection through appressoria formation. Subsequently, plants were grown in a growth chamber under 16-h day light at 20°C.

2.2 Isolation and enrichment of haustoria

Leaf material was harvested on 6 days after inoculation just before sporulation, following a dark cycle; only sections showing yellowing were taken and leaf surfaces were wiped

clean of remaining urediniospores with a gloved finger. Haustoria were enriched over sucrose gradients; all steps were performed on ice or at 4°C, following a modified procedure of Tiburzy et al. [27]. Briefly, 20 g of leaves was cut into 2 cm lengths in buffer M (0.1 M K-phosphate, pH 6.7, 0.1 M sucrose, 1.5 mM $MgSO_4$, 1.0 mM PMSF), homogenized in a blender and filtered through 100 μm pore size nylon mesh (Nitex Nylon, LAB PAK, Sefar America, Depew, NY, USA). The filtrate was centrifuged for 10 min at $3000 \times g$ in a swinging bucket rotor (SH3000, Sorvall). The supernatant was removed and 10 mL of buffer M was added, mixed gently and then filtered through a 25-μm pore size nylon mesh (Nitex). The sample was then re-centrifuged at 380 g for 10 min. The supernatant was aspirated off and the pellet resuspended in 7 mL of buffer M. The resulting suspension was pipetted onto a sucrose gradient in 0.1 M phosphate buffer in 30 mL silanized glass centrifuge tubes using the following steps: (all sucrose percentages are w/v) 60%, 1.7 mL; 55%, 3.4 mL; 50%, 3.6 mL; 45%; 3.7 mL; 40%, 5.0 mL; 30%, 7.7 mL. This gradient was centrifuged at $3000 \times g$ for 8 min in the same rotor as before with the brake and acceleration set to 2 (Sorvall Evolution Centrifuge). The top two layers of sucrose were removed and discarded, and the remaining solution mixed and divided into three 30 mL glass centrifuge tubes. To each tube, 10 mL of buffer M was added and all three were centrifuged at $3000 \times g$ for 7 min. The pellet was resuspended in 10 mL of buffer M and re-centrifuged at $3000 \times g$ for 5 min. The pellets were resuspended in 3 mL of buffer M, layered onto the same sucrose gradient as before, repeating the centrifugation and subsequent wash steps. The final pellets were resuspended in a total of 3 mL buffer M and layered onto a single sucrose gradient in one 15 mL glass centrifuge tube, such that each step was the same height as in the 30 mL tube (i.e. 60%, 1.0 mL; 55%, 2.0 mL; 50%, 2.0 mL; 45%, 2.0 mL; 40%, 2.5 mL; 30%, 3.0 mL). This was centrifuged as previously and the 40–55% layers containing the enriched haustoria fraction were collected and pooled. A small sample was removed for microscopic analysis by staining with calcofluor M2R White [28].

2.3 Verification of haustorial enrichment

Amplification, data acquisition and data analysis were carried out using the CFX96™ Real-Time PCR Detection System (Bio-Rad). qPCR quantitation of fungal biomass was based on a procedure for quantifying *Magnaporthe oryzae* biomass in rice [29]. Genomic DNA extractions from heavily infected leaves and enriched haustorial fractions were performed using the DNeasy Plant Mini Kit (Qiagen). *PtRTP1* (PTTG_03497, coding for a 210-amino-acid protein) and *Ta-psbA* (GenBank accession no.: AB042240) were used as marker genes to quantify *Pt* gDNA and wheat chloroplast DNA, respectively. To establish quantification, DNA fragments representing *PtRTP1* and *Ta-psbA* were obtained by PCR using primer pairs RTP1F/RTP1R and psbAF/psbAR, respectively (Table 1). PCR products of 222 and 297 bp were cloned in vector pENTR™/D-TOPO (Invitrogen), yielding plasmids pENTR-RTP1 and pENTR-psbA, respectively. These plasmids, purified using EZ-10 Spin Column Plasmid DNA Kit (Bio Basic, Canada), were diluted to a concentration of 5×10^{10} molecules/μL. Different standard dilutions for pENTR-RTP1 or pENTR-psbA were prepared ranging from 10^3 to 10^{10} molecules/μL. From these standards, linear regression models were established, linking observed C_t values with log 10 target concentration. These models were used to calculate the number of target DNA copies in the experimental samples from the observed C_t values, based on obtained correlation coefficients and efficiencies (R^2; data not shown). To measure the changes in the expression of *Pt-RTP1*, qRT-PCR was used. From the same samples, RNA was extracted and cDNA prepared as in Section 2.7. The relative differentially expressed ratio of *Pt-RTP1* was

Table 1. Primers used in quantitative PCR assays

Gene/*Pt* unigene/EST	Forward primer	Reverse primer
Pt-RTP1	CGGAAGAATAGCCGGAAAATG	CTTAGACATCTCGATGTCTCG
Ta-psbA	TTCCAGGCAGAGCATAACATC	CCAGATTCCTACTACAGGCCAA
Pt-polyubiquitin	GCACGCTCTCTTCATTTGTG	TTGACACGAGATCGTTGCTT
Pt-α-tubulin	GAGATGACCATGTCCTGCTTCGA	GACTGACTTTGGCGGTGTCTGA
Pt-succinate dehydrogenase	GGTTCCAGCGATAGATCGAG	CAACTACGACCAGCCACTCA
PtContig306	GAAGCATCATTTCCACCACA	GACGCAAATGGTGAATTCCT
PTTG_00925	AGCGGTGGTCTGATGAAAAC	TGTCTTCCTTTGGCATCCAT
PTDH.cn565.na.ptih	GTACAGCTGCACTGGGGAAT	GCAGGGTCATCCATCCTAAC
PtContig2863	TGTCAGCTTTCGATCCTCCT	TGATCTTCGGAAAGCGAGTT
PtContig2570	GCAACATCCACCTGTACTCG	ATGATCGCCTTGAAACATCC
PTTG_05834	CTCGCCCTCGCTAACAGTAA	CTCGGCGTTTTCCTTTTGT
PTTG_03653	GAAGCATCATTTCCACCACA	GACGCAAATGGTGAATTCCT
PTTG_06270	GGAAATGAAGGACCACATGC	AGCGAGGGTAGCTCTGAATG
PTTG_04892	TCAGTCCTGTTGCTCGATTG	CGGTTTGCCAGAGTCCTAAG
PTTG_06324	CATCATCCTCCAACCTTCCT	TGGTGAAAACAGTGGCTGTG

calculated and normalized to the level of expression of *Pt*-polyubiquitin automatically by the CFX manager software with a $\Delta\Delta C$(t) mode selected.

2.4 Generation of protein profiles, 2-D gel

Samples were prepared for 2-DE as described previously [30]. Briefly, enriched haustoria were first centrifuged to remove sucrose; the pellet was then frozen at -20°C for 1 h prior to the addition, with vortexing, of ice-cold acetone containing 10% w/v trichloroacetic acid (TCA) and 0.07% w/v DTT. After precipitation, the pellet was washed extensively with acetone containing 0.07% w/v DTT. The final pellet was redissolved in isoelectric focusing (IEF) solution and proteins separated by IEF × SDS-PAGE exactly as described [30] on 24-cm IEF strips (pH 4–7; GE Healthcare) and 12% SDS-PAGE. Gels were stained with Coomassie brilliant blue R-250 and scanned to produce TIF images. Proteins were identified from tryptic peptides by mass spectrometry as described by Rampitsch and Bykova [31].

2.5 GeLC-MS

For GeLC-MS, proteins were separated by SDS-PAGE. Standard Tris-glycine and Tris-tricine gels were run using 10–18% gradient gels set up in 0.75 mm × 180 mm plates (SE600: Hoefer). In the first set of experiments (one Tris-glycine and Tris-tricine gel), only bands containing proteins that were differentially expressed between oil-inoculated and wheat leaf rust (WLR)-infected samples were excised from gels with a scalpel. In the second set of experiments (Tris-glycine gels only), the entire gel lane was sliced up into 10 parts of approximately equal size. For each set of experiments, two biological replicates were prepared for each interaction (infected leaves and oil inoculation), and two technical replicates were run for each sample. Proteins were digested in situ with modified sequencing grade trypsin (Invitrogen). Tryptic peptides from gel slices were analyzed by reversed-phase nanoscale LC (LC; Ultimate 3000: Dionex, Germany) coupled to a linear ion-trap mass spectrometer (LTQ: Thermo Finnigan, San Jose, CA, USA). A 10-cm C_{18} column (5 μm particle/300 Å pores) was prepared in-house and used to introduce peptides into the mass spectrometer via nano-spray ionization at 250 nL/min using a 2–80% v/v ACN gradient in 1% v/v formic acid (FA), 0.5% v/v acetic acid over 65 min. The LTQ was programmed to produce a full survey scan (m/z 400–2000) to select the five most abundant ions from this and perform, serially, an MS^2 scan on each. Former precursor ions were excluded from the analysis for 36 s. Collision energy for MS^2 was 28.0 (isolation width 2.5), tuned with [Glu1]-fibrinopeptide B ($m/z = 1570$).

2.6 Generation of database and data analysis

Two databases were compiled: one comprised a set of 11 630 proteins predicted from the preliminary *Pt* genome sequence, a set of over 6000 compiled *Pt* EST unigene sequences (Xu, Linning, Borodovsky, Fellers, Dickinson, Bakkeren et al., unpublished data; sequences deposited in GenBank) and a set of 20 567 predicted *Pgt* proteins. A second database comprised the National Centre for Biotechnology Information (NCBI) non-redundant database limited to *Viridiplantae*. Output files were queried separately against these two databases using MASCOT (v2.2, Matrixscience, UK [32]). Proteins were considered to be matched correctly if two or more peptides were returned by MASCOT with a statistically significant score ($p < 0.05$ of random assignment). All searches were repeated with a decoy (reversed) database which returned false discovery rates of $<2\%$ for both databases. The following settings were used for MASCOT. Fixed modification: carbamidomethyl (C); variable modifications: deamidation (NQ), oxidation (M); no quantitation; peptide tolerance was set to ± 2.0 Da, and MS^2 tolerance to ± 0.8 Da; monoisotopic peptides with charged states of +1, +2 and +3 were queried using the ESI-Trap instrument parameters (i.e. using *b*- and *y*-ion series). MASCOT 'MuDPIT' scoring was used: only peptides with a significant score contributed to the overall score of the return. Protein motif and cellular localization searches were performed with TargetP [33], SignalP 3.0 [34], TMHMM 2.0 [35] and Wolf PSORT [36]. Furthermore, because TMHMM may not distinguish signal peptides from transmembrane domains, deduced proteins with a single transmembrane domain within 40 amino acids of the N-terminus were also considered as potential secreted proteins [37].

2.7 qRT-PCR analysis

Total RNA was isolated from freshly frozen cell material by grinding with sterile sand and extraction in a solution of phenol-guanidine isothiocyanate ('TRI Reagent', BIO/CAN Scientific) according to instructions provided by the manufacturer. RNA was treated with TURBO™ DNase (Ambion) for 60 min at 37°C, extracted with phenol/chloroform and then precipitated overnight at -80°C by adding 1/10 volumes of 3 M sodium acetate, pH 5.3, and $2^{1/2}$ volumes of 96% ethanol. Two micrograms of total RNA was used to synthesize first-strand cDNA using oligo $(dT)_{15}$ primer with M-MuLV RNase H^+ reverse transcriptase (Finnzymes) according to the manufacturer's instructions. qRT-PCR was performed on a CFX96™ Real-Time PCR Detection System (Bio-Rad) with primer pairs as indicated in Table 1. Transcript levels were derived from the accumulation of green fluorescence using the following reaction set up: 5 μL volume 1 × SsoFast Evagreen Supermix (Bio-Rad) containing 200 nmol of each primer and 0.25 ng cDNA (based on input RNA), using the following profile: 2 min at 95°C; 40 cycles of 10 s at 95°C, 30 s at 55°C. The C_t values for each

gene were converted to amounts of cDNA present in the sample relative to a standard curve of C_t values for each gene generated by serial dilutions of known quantities of total *P. triticina* genomic DNA, using the same PCR cocktail. Based on the occurrence in the EST database and preliminary expression data from cDNA microarray experiments, five gene candidates were tested for suitability as reference genes. *Pt* polyubiquitin (PtContig7422, GenBank TSA accession no.: EZ116190), α-tubulin (PtContig2591, EZ116163) and succinate dehydrogenase (PtContig7907, EZ116204) were selected as reference genes, verified by GeNorm analysis (http://medgen.ugent.be/~jvdesomp/genorm/) to be the most invariably expressed among the tissues sampled. Amounts of qPCR product were subsequently normalized to the geometric mean of the amount of *Pt* polyubiquitin, α-tubulin and succinate dehydrogenase products. RNA was extracted from three independent biological replicate experiments, and each PCR product was evaluated in at least two independent experiments, including two technical replicates.

2.8 Accession numbers

Sequences of identified *Pt* and *Pgt* proteins and corresponding genes can be found on the website of the Broad Institute of MIT, Cambridge, MA (http://www.broadinstitute.org/annotation/genome/puccinia_group/MultiHome.html, *Pgt* built July 2007, *Pt* built November 2009). The identified Ptcontig (assembled) and constituent and/or singlet EST sequences are available from NCBI at the Transcriptome Shotgun Assembly Sequence Database (http://www.ncbi.nlm.nih.gov/Genbank/TSA.html) or at dbEST (http://www.ncbi.nlm.nih.gov/sites/entrez?db = nucest [6]), respectively.

3 Results

3.1 Haustorial purification

Ultrastructural studies of haustoria in *Puccinia* species within compatible cereal hosts reveal flask-, cigar- and older,

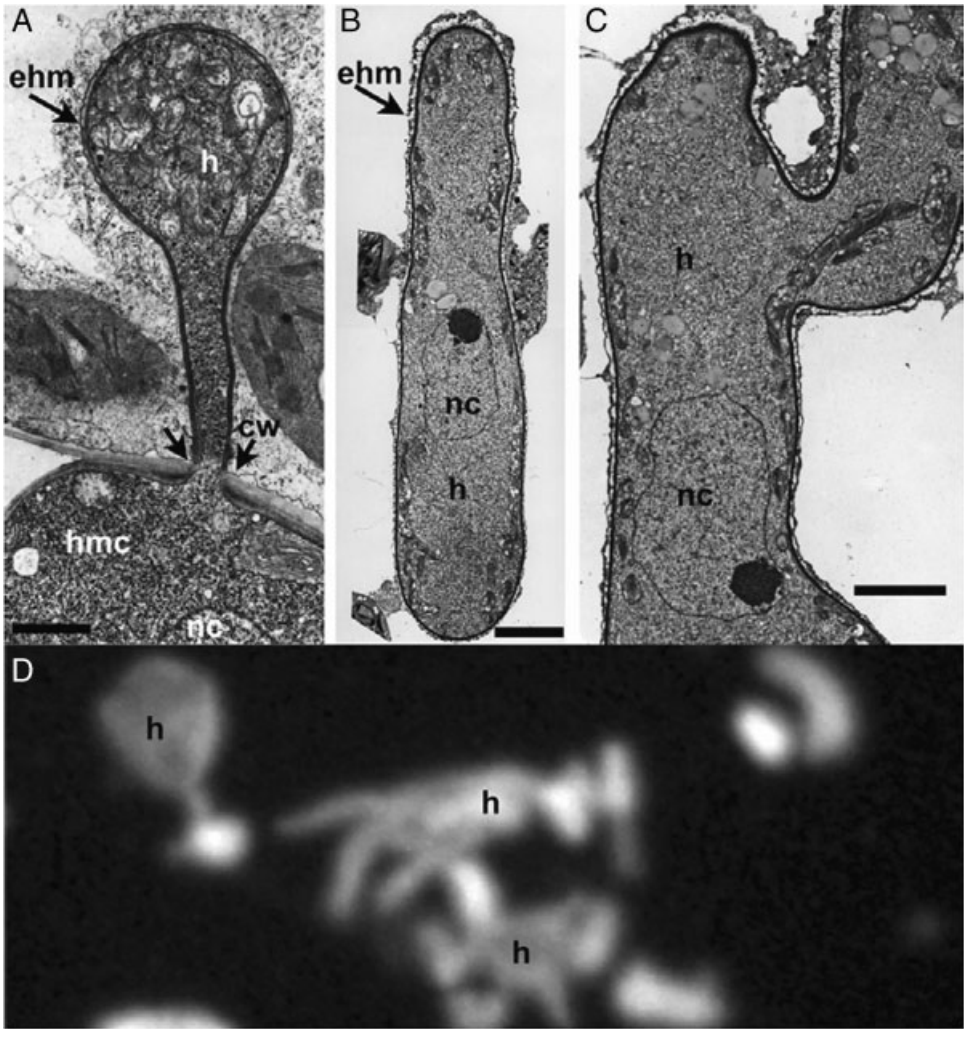

Figure 1. Transmission electron microscopy of in situ haustoria in infected wheat (A) and oat (B, C), and fluorescence microscopy of a haustorial preparation from infected wheat enriched over sucrose gradients (D). (A) Formation of a young, flask-shaped haustorium (h) of *P. graminis* f. sp. *tritici* after a haustorial mother cell (hmc) has breached the host cell wall (cw, double arrows). Note the invagination of the host plasmalemma to form the extra-haustorial membrane (ehm) surrounding the haustorium (single arrow). The hmc nuclei (nc, only part of one shown) have not yet migrated into the haustorium. Scale bar = 1 μm. (B) Older, cigar-shaped and (C) branched mature haustoria (h), of *P. coronata* nc, nucleus. Scale bar = 2 μm. (D) Calcofluor-stained sample of enriched *P. triticina* haustoria (h) after sucrose gradients (see Section 2, field of view shows a young, flask-shaped haustorium and two older, branched haustoria). Images illustrate haustoria from infections from three different *Puccinia* species but haustoria found in infected cereal plant cells are very similar in morphology [83].

branched-shaped bodies within host cells surrounded by an invaginated host plasma membrane (Fig. 1A–C); a dark-staining 'neck band' demarcates the entry point near the breached cell wall [38, 39]. Several procedures exist for the specific enrichment of haustorial structures from rust fungus-infected plants. We harvested heavily infected leaves from young plants approximately 6 days after inoculation just before sporulation as the starting material (see Section 2). This time point is a compromise between convenience to obtain sufficient amounts of haustoria (significant loss occurs during purification) and biological relevance. Arguably, crucial steps in the establishment of the infection take place during the first 48 h when many secreted effectors might be released; but since the infection is not deemed very synchronous and since new haustoria will be formed by the mycelium while traveling through the plant tissues, it was reasoned that a representative proteome could be obtained at 6 days after inoculation.

To obtain haustorial preparations, we initially used filtration through nylon mesh filters followed by affinity chromatography over columns charged with the lectin concanavilin A (Con A). This method, based on the specific surface qualities found in haustoria from different rusts, was pioneered by Hahn and Mendgen [40] and has been used by many researchers. However, in our hands haustorial enrichment at $<20\%$ among chloroplasts was deemed not sufficient. Although quite successful for subsequent RNA extraction and stage-specific cDNA library construction (e.g. for the generation of ESTs), we were not successful in obtaining clear separations after protein extractions and two-dimensional gel analyses. We subsequently used a method based on filtration and sucrose density centrifugation of infected plant material [27]. These samples showed better enrichment of haustorial structures of at least 40% among chloroplasts (Fig. 1D); other fungal structures such as mycelia (runner hyphae) were found in other fractions of the sucrose gradient and did not co-purify with the haustoria. Experiments to increase purity involved further rounds of centrifugation, however, at the cost of yield loss and probable deterioration of the proteome (and transcriptome) of the haustoria. Therefore, we chose an intermediate level of haustorial purification, also because many host chloroplast proteins are known allowing identification of those contaminating proteins among the MS/MS-derived proteome data.

To validate the enrichment procedure, we designed and conducted two molecular tests based on qPCR analysis. In calcofluor-stained samples of enriched *Pt* haustoria, we found chloroplasts to be the main contaminants. We developed primers for a wheat chloroplast genome-specific DNA marker, the *Ta-psbA* gene, and for a *Pt*-specific, single copy gene, *PtRTP1* (rust transferred protein 1). qPCR was performed on total DNA isolated from the whole infected leaf samples used as the starting material, and from the final haustoria-enriched fractions. Figure 2A shows that the fraction of fungal genomes to wheat chloroplast genomes

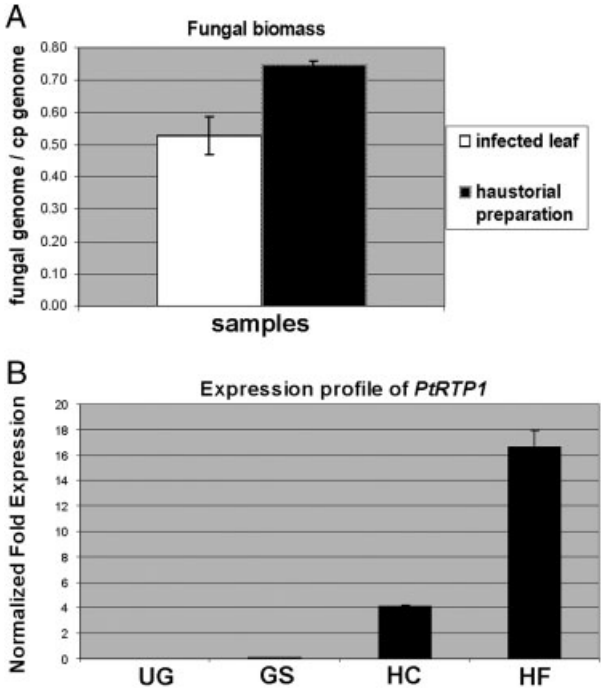

Figure 2. Validation by qPCR of the haustoria enrichment procedure. (A) Fungal biomass was calculated as the ratio of fungal nuclei per chloroplast genomes using single gene markers *Pt-RTP1* and *Ta-psbA*, respectively, on total genomic DNA preparations. (B) qRT-PCR analysis on cDNA. Expression profile of *Pt-RTP1* in samples of resting urediniospores (UG), urediniospores germinating over water (GS), total infected leaf starting material (HC) and the enriched haustorial fraction (HF).

increases by 44% during the enrichment procedure. For the second test, we searched for a gene specifically expressed in haustoria. The bean rust fungus, *Uromyces fabae Uf-RTP1* gene was originally isolated from a haustorium-specific cDNA library and identified as in planta-induced gene *PIG7* by Hahn and Mendgen [41]. This gene was subsequently shown to be expressed exclusively in haustoria and its protein product was transferred from the extra-haustorial matrix to the host nucleus [42]. Its homolog from *Uromyces appendiculatus*, *Ua-RTP1*, has been used to demonstrate haustorium-specific enrichment of fungal RNA over plant RNA [43, 44]. We identified a single homolog in *Pt*, *PtRTP1*, and measured by qRT-PCR its expression in resting urediniospores, urediniospores germinating in vitro over water, in the infected wheat leaf starting material and in the haustorial-enriched fractions. Figure 2B shows that *PtRTP1* is exclusively expressed during infection. Moreover, the abundance of *PtRTP1* transcripts is more than fourfold higher in the haustoria-enriched fraction than in the infected leaf homogenate. Although we have not demonstrated that, in analogy with *Uf-RTP1*, *PtRTP1* is expressed exclusively in haustoria, among the 44 000 ESTs we generated, we identified three ESTs representing this gene in only the cDNA library constructed from isolated haustoria. This fact

and the quantitative molecular data as presented in Fig. 2, in combination with microscopic observations that virtually no mycelial fragments co-purify in our purification scheme, suggest that we have obtained mainly haustorial fungal structures with a fraction of chloroplasts.

3.2 Building the reference database

The *Pt* genomic resources being developed at the Broad Institute, Cambridge, MA (C. Cuomo in collaboration with J. Fellers, L. Szabo and G. Bakkeren), allowed the generation of a preliminary proteome of 11 630 predicted proteins. In addition, an initial database of over 25 000 ESTs [6] was expanded to over 40 000 EST sequences. These covered various *Pt* life cycle and developmental stages such as resting urediniospores, urediniospores germinated in vitro over water and infections in wheat and on the alternate host. A large number of ESTs (more than 11 000) were generated from heavily infected wheat leaves and isolated haustorial preparations, the latter of which represents the fraction corresponding to the haustorial proteins to be matched in the current study. Assembly and analysis using *Pgt* fungus-trained gene calling and sanitation against preliminary *Pt* genome reads, generated over 6000 predicted fungal, non-redundant unigenes from the expanded set (Section 2). A near-comprehensive set of 20 567 proteins predicted from the related *Pgt* genome sequence was also used for searching (Section 2).

3.3 2-D gel analysis

Initially, we generated 2-D gels resulting in the identification of only 30 proteins from 25 spots in the samples from infected leaves that contained protein(s) that accumulated to higher amounts in infected leaves than in leaves treated with oil (Supporting Information Fig. S1). In most spots, a single protein was detected, possibly with the exception of spots 12, 13, 16, 17, 18, 19 and 20. Of the 30 identified proteins, 17 were likely of fungal origin (Table 2 and Supporting Information Table S1, protein IDs marked with an asterisk). Since the resolution of the proteins was limited, as was the number of identified proteins, we proceeded with the GeLC-MS technique which identified all the fungal proteins from the 2-D analysis except two: PTTG_09553 and PTTG_01827.

3.4 GeLC-MS analysis

One of the advantages of the GeLC-MS technique over the 2-D gel approach is that 2% w/v SDS can be used during tissue extraction. This solubilizes many proteins, including membrane-associated ones and presumably ones embedded in the extra-haustorial matrix; it simultaneously inhibits the action of many proteases. Material from two biological replicate plant inoculations was analyzed on standard Tris-glycine and Tris-tricine gels; the latter was used to better represent low molecular weight proteins (below 15 kDa). Figure 3 shows a representative Tris-glycine gel whose lanes were divided into ten slices for analysis.

Mass spectra generated from the GeLC-MS experiment were queried against the rust-specific and the NCBI-*Viridiplantae* databases (see Section 2). The mass spectra from the *Pt*-infected peptide mixtures returned over 260 fungal proteins, mostly from the *Pt* genome predicted proteome, 20 from the *Pt* EST unigene set (14 contigs and 6 singlets) and 16 were identified among homologs in the predicted *Pgt* proteome (Table 2 and Supporting Information Tables S1 and S2). The fact that some *Pt* spectra matched peptide sequences in *Pgt* reflects conservation between these two cereal rust species (corroborated by comparative gene and EST studies; Fellers, Borodovsky, Dickinson, Bakkeren et al., unpublished data).

3.5 Functional classification

The annotated proteins were tentatively classified into 13 categories according to groupings used in the Kyoto Encyclopedia of Genes and Genomes (KEGG [45]). A relatively high percentage of proteins was classified in the energy and (general) metabolism categories (86 proteins or 33%), whereas 64 (24%) were put in the 'Translation' category with 53 of them annotated as ribosome structural proteins. Another category with a relatively high number of annotated proteins comprised 40 proteins with binding/folding/protecting activities such as heat-shock proteins (HSPs)/chaperones, and 6 possibly involved in the proteasome degradation pathway. The category 'Protein Export' (eight proteins or 3%) included endoplasmic reticulum proteins but SEC proteins could possibly have functions in the molecular machinery for effector translocation/secretion. A relatively large group of 31 proteins (12%) could not easily be classified within KEGG with 17 proteins returning no annotation upon searching various databases.

3.6 Secreted protein prediction

Since the haustorium is a major hub of activity with protein and metabolite trafficking between it and the host cytoplasm, one of the goals of this study is to reveal the actual 'secretome'. In order to obtain the most accurate prediction of secreted proteins, we subjected the proteins identified in this proteomic analysis to multiple prediction programs and compared them with a variety of resources identified in other pathosystems. Firstly, proteins were analyzed using Wolf PSORT (http://wolfpsort.org/) for domains or motifs that would indicate their targeting and/or cellular localization (Table 2, column 'Localization'). Secondly, in silico predictions were

Table 2. *Puccinia triticina* proteins identified by GelC-MS

Protein description[a)]	Protein ID[b)]	No. of peptides matching	MASCOT score	Localization[c)]	Secreted[d)]
Amino acid metabolism					
2-Oxoglutarate dehydrogenase	PGTG_02140	2	94	Cysk	
2-Oxoglutarate dehydrogenase	PTTG_04398	3	89	?	
2-Oxoglutarate dehydrogenase E1	PTTG_06893	6	243	Mito	
6-Phosphogluconate dehydrogenase	PTTG_00183	2	120	Extr	
6-Phosphogluconate dehydrogenase	PTTG_03422	2	120	Extr	
Aminomethyltransferase	PTTG_02595	2	116	Mito	
Aspartate aminotransferase	PTTG_01749	9	871	Mito	
Carbamoyl-phosphate synthase L_chain	PTTG_02278	2	101	Mito	
Dehydrogenase	PTTG_07476*	9	663	Mito	
Disulfide oxidoreductase	PTTG_01369	4	171	Mito	
Glycine dehydrogenase	PTTG_09874	2	100	?	
Glycine hydroxymethyltransferase	PTTG_00829	16	1237	Mito	
Homoaconitate hydratase	PTTG_04573	3	102	Mito	
Ketol-acid reductoisomerase, fungal type	PTTG_01858	6	817	Mito	
Leucine aminopeptidase 2	PTTG_00586	2	66	Extr	
N-acetylglutamate synthase	PTTG_01263	3	121	Mito	
N-acetylglutamate synthase	PTTG_01874	3	121	Mito	
Pyruvate dehydrogenase complex α chain	PTTG_01684*	4	165	Mito	
Saccharopine dehydrogenase	PGTG_06954	2	295	Cyto	
Saccharopine dehydrogenase	PTTG_09770	2	77	Cyto	
Carbohydrate metabolism					
Aconitase	PTTG_02579	5	125	Mito	
Alcohol dehydrogenase	PTTG_01381	2	123	Cyto	
Aldolase	PTTG_06440	11	485	Cyto	
Aspartate ammonia lyase	PTTG_04108	10	447	?	
ATP-grasp_2	PTTG_08248*	9	549	Mito	
Chitinase	PTTG_01527*	3	150	Extr	Yes
Chitinase	PTTG_05954	4	179	Extr	Yes
Citrate synthase	PTTG_09412	3	254	Mito	
Dihydrolipoamide acetyl/succinyl-transferase	PTTG_06313	2	103	Mito	
Dihydrolipoamide succinyltransferase	PTTG_09731*	5	213	Mito	
Enolase	PTTG_00430	3	202	Cyto	
Glucan 1,3 β-glucosidase protein	PTTG_06164	2	128	Extr	
Glyceraldehyde 3-phosphate dehydrogenase	PTTG_08295	9	795	Cyto	
Glycerol-3-phosphate dehydrogenase	PGTG_17260	2	383	Mito	
Glycerol-3-phosphate dehydrogenase	PTTG_01531	17	796	Mito	
Malate and lactate dehydrogenase	PTTG_01833	2	264	?	
Malate dehydrogenase	PTTG_01563	12	927	Mito	
Mannosyl oligosaccharide glucosidase	PTTG_09087	10	461	Extr	Yes
Methylenetetrahydrofolate dehydrogenase	PTTG_03475	3	151	?	
NAD+-specific isocitrate dehydrogenase	PTTG_00041	8	1307	Mito	
NAD+-specific isocitrate dehydrogenase	PTTG_00042	3	301	Mito	
NADH-cytochrome B5 reductase	PTTG_05129	5	251	Mito	
NADH-cytochrome B5 reductase	PT0113c.D02.BR.ptg (EC414365)	3	208	?	
Phosphoglycerate kinase	PT0133c.C09.BR.pth (EC415693)	4	366	Cyto	
Pyruvate kinase	PTTG_08360	3	105	Cyto	
Seven-hairpin glycosidases	PTTG_00839	2	74	Extr	Yes
Succinate dehydrogenase 2 flavoprotein subunit	PTTG_05785	2	83	Mito	
Succinate dehydrogenase iron-sulfur protein	PTTG_01208	2	80	?	
Succinate-semialdehyde dehydrogenase	PTTG_09575	4	173	Mito	
Succinyl-CoA synthetase	PTTG_07355	5	256	Mito	

Table 2. Continued

Protein description[a)]	Protein ID[b)]	No. of peptides matching	MASCOT score	Localization[c)]	Secreted[d)]
Transaldolase	PtContig7447 (HP458645)	2	89	Cyto	
Trehalose phosphatase	PTTG_07988	2	84	Extr	Yes
Triosephosphate isomerase	PTTG_02613	3	147	Cyto	
Oxidative phosphorylation					
ATP synthase	PGTG_15605	7	770	Mito	
ATP synthase	PTTG_01840*	13	1380	Mito	
ATP synthase δ chain	PTTG_03075	6	230	Mito	
ATP synthase F1	PTTG_00521	9	538	Mito	
ATP synthase γ chain	PtContig5661 (EZ116182)	9	522	Cyto	
ATP_subunit_h	PTTG_02983	2	119	Mito	
ATP-citrate synthase	PTTG_02126	6	130	Mito	
Cytochrome *c* oxidase 5B	PTTG_02082	2	160	Mito	
Cytochrome *c*1	PTTG_04815	3	163	Mito	
Cytochrome II	PTTG_30014	2	106	Mito	
Cytochrome-*c* oxidase	PTTG_00348	2	97	Mito	
Electron transfer flavoprotein α-subunit	PTTG_04265	3	165	Cyto	
FAD-dependent oxidoreductase	PTTG_02950	2	82	Extr	
Inorganic pyrophosphatase	PTTG_03429	2	51	?	
Metalloprotease	PTTG_01903*	6	274	Mito	
Mitochondrial ATP synthase B chain	PTTG_08325	2	84	Mito	
Mitochondrial ATP synthase B chain	PtContig95 (HP451905)	3	148	Extr	Yes
NADH dehydrogenase flavoprotein 1	PTTG_04129	2	167	Mito	
NADH-ubiquinone oxidoreductase	PGTG_10555	2	114	Mito	
NADH-ubiquinone oxidoreductase	PTTG_03798	2	153	Mito	
NADH-ubiquinone oxidoreductase	PTTG_06046	9	491	Mito	
NADH-ubiquinone oxidoreductase	PTTG_06874	2	98	Mito	
NADH-ubiquinone oxidoreductase 39 kDa subunit	PTTG_01620	5	214	?	
NADH-ubiquinone oxidoreductase-related	PTTG_07896	2	120	Mito	
NADPH cytochrome P450 reductase	PTTG_03033	3	134	Plas	
Plasma membrane H+ transporting ATPase 1	PTTG_05531	19	493	Plas	
Subfamily not named	PTTG_07870	2	134	Mito	
Subunit VIa of cytochrome *c* oxidase	PtContig8060 (HP459199)	2	127	Mito	
Superoxide dismutase 2	PTTG_05861	2	136	Mito	
Thioredoxin	PTTG_01431	3	138	Mito	Yes
Ubiquinol–cytochrome *c* reductase	PTTG_03576	2	477	?	
Ubiquinol–cytochrome *c* reductase	PTTG_09811	2	477	?	
Ubiquinol–cytochrome *c* reductase iron-sulfur subunit-related	PTTG_07225	4	456	?	
Folding, sorting and degradation					
25 kDa subunit of signal peptidase complex, SPC25	PTTG_09840	4	242	?	
26S proteasome non-ATPase regulatory subunit 1	PTTG_05719	2	59	Nucl	
26S proteasome regulatory subunit	PTTG_08733	2	135	Plas	
26S proteasome regulatory subunit RPN2	PGTG_06912	2	79	Cyto	
ADP-ribosylation factor	PTTG_02596	3	107	Mito	
ATP-dependent protease La	PGTG_13980	5	208	?	
ATP-dependent protease La	PGTG_06421	5	208	?	
Aspartyl protease	PtContig7957 (HP459118)	3	269	Cyto	
Carboxypeptidase cpdS precursor	PTTG_06087	2	111	Extr	
Chaperone protein dnaK	PTTG_01803	18	1330	Nucl	
Chaperone protein dnaK	PTTG_01076*	17	2158	Mito	
Chaperonin 10	PTTG_05826	2	59	Mito	
Chaperonin 60	PTTG_05827*	6	333	Mito	
Clathrin heavy chain	PTTG_01415	2	78	?	

Table 2. Continued

Protein description[a)]	Protein ID[b)]	No. of peptides matching	MASCOT score	Localization[c)]	Secreted[d)]
Cyclophilin, peptidyl-prolyl *cis–trans* isomerase	PTTG_01372	2	89	Extr	Yes
Cyclophilin, peptidyl-prolyl *cis–trans* isomerase	PTTG_04303	2	89	Extr	Yes
Cyclophilin, peptidyl-prolyl *cis–trans* isomerase	PTTG_02119	2	158	Mito	
Heat-shock protein 70	PTTG_01222	2	68	Mito	
Heat-shock protein 70	PTTG_06787	3	125	Cyto	
Heat-shock protein 70	PTTG_07281*	12	860	Extr	Yes
Heat-shock protein 70	PTTG_01696*	3	158	Cyto	
Heat-shock protein 70	PTTG_03478*	5	260	Cyto	
Heat-shock protein 90	PTTG_06867	3	152	Nucl	
Heat-shock protein 90	PTTG_00140	10	453	?	Yes
Import inner membrane translocase subunit tim44	PTTG_04574	3	121	Mito	
Metalloprotease	PTTG_02620*	4	305	Mito	
Mitochondrial import receptor subunit TOM40	PTTG_00312	3	159	Nucl	
Polyubiquitin	PTTG_01748	2	192	Cyto_nucl	
Polyubiquitin	PTTG_11442	2	192	Cyto_nucl	
Polyubiquitin	PTTG_11572	2	192	Mito	
Prohibitin, involved in determination of replicative lifespan	PGTG_00454	6	427	?	
Prohibitin, involved in determination of replicative lifespan	PTTG_10202	3	56	Cysk	
Protease IV, Ssp	PTTG_00896	7	375	?	
Protein disulfide isomerase	PTTG_00495	5	357	Extr	Yes
Protein disulfide isomerase	PTTG_01827* ♯	10	937	Extr	Yes
Subtilisin	PTTG_05438	2	134	?	
Subtilisin-like serine protease	PTTG_05451	2	121	Extr	Yes
Surfeit locus protein Surf4	PTTG_06998	2	175	Plas	Yes
Vacuolar dynamin-like GTPase VpsA	PGTG_15816	3	177	Cyto	
Zinc metalloprotease	PTTG_05241	2	99	?	
Protein export					
Coatomer protein	PTTG_00410	3	132	?	
Endoplasmic reticulum protein	PTDH_P002.D16.r1.pth (GR505099)	2	121	?	Yes
ER protein translocation complex component Sec63	PTTG_08452	3	109	Cyto	
Preprotein translocase SECY subunit (SEC61)	PTTG_02940	2	105	Plas	
Protease family S26 microsomal signal peptidase subunit SPC18,21/SEC11	PTTG_04259	2	105	Extr	
Protein transport protein SEC13	PTTG_05744	3	148	?	
Protein transport protein SEC31	PTTG_03860	2	72	Mito	
SEC24-related protein	PTTG_05733	3	110	Nucl	
Metabolism of cofactors and vitamins					
Pyridoxine biosynthesis protein Pdx1	PTTG_09373	3	255	Mito	
Thiamine biosynthesis protein NMT1	PTTG_05201	3	140	Cyto	
Thiamine biosynthesis Thi4 protein	PGTG_01304	4	539	Cyto	
Thiazole biosynthetic enzyme	PtContig280 (HP452059)	6	1080	?	
Replication and repair					
Actin	PTTG_03323	2	98	Cysk	
Cell division cycle protein 48	PTTG_01623	2	144	?	
DNA helicase TIP49, TBP-interacting protein	PTTG_09553* ♯	6	363	Mito	

Table 2. Continued

Protein description[a)]	Protein ID[b)]	No. of peptides matching	MASCOT score	Localization[c)]	Secreted[d)]
H15 superfamily member, histone 1	PTTG_08265	2	115	Mito	
HistoneH2A	PTTG_04461	2	146	Nucl	
HistoneH2A	PTTG_00333	2	146	Nucl	
HistoneH2B	PTTG_05040	3	340	Nucl	
Signal transduction					
Calreticulin	PTTG_00276	2	98	Cyto	
Casein kinase II α chain	PTTG_07780	3	159	?	
RNA binding and modification					
Arginine/serine-rich splicing factor	PGTG_07555	2	220	Nucl	
Argonaute-like protein	PTTG_07511	2	98	Mito	
ATP-dependent RNA helicase	PTTG_06915	11	646	Mito	
RNA12 protein, nucleic acid binding	PTTG_08189	2	93	?	
RNA-binding protein	PTTG_05797*	5	979	Mito	
RNA-binding protein	PTTG_05122	2	115	Mito	
Transformer-2-related	PTTG_06790	2	76	Nucl	
Translation					
30S/40S ribosomal protein S4	PTTG_04832	3	150	Cyto	
40S ribosomal protein S11	PGTG_04599	2	91	Mito	
40S ribosomal protein S13	PTTG_04426	2	134	Nucl	
40S ribosomal protein S17	PTTG_04537	3	365	Mito	
40S ribosomal protein S18	PTTG_01401	3	112	?	
40S ribosomal protein S19	PTTG_05323	2	123	Cyto	
40S ribosomal protein S2	PTTG_06873	3	230	Cyto	
40S ribosomal protein S20	PTTG_09968	2	123	Cyto	
40S ribosomal protein S24	PTTG_06914	3	156	Mito	
40S ribosomal protein S27	PTTG_08260	2	148	Mito	
40S ribosomal protein S3	PTTG_00689	4	108	Mito	
40S ribosomal protein S3A	PTTG_03521	4	130	Nucl	
40S ribosomal protein S5	PTTG_00123	2	144	?	
40S ribosomal protein S5	PTTG_02129	2	144	Mito	
40S ribosomal protein S7	PTTG_03711	3	196	?	
40S ribosomal protein S8	PTTG_05114	2	93	Nucl	
40S ribosomal protein S8	PTTG_06328	3	196	?	
40S ribosomal protein S9	PGTG_07099	2	108	Nucl	
60S acidic ribosomal protein	PTTG_03284*	7	723	Cyto	
60S acidic ribosomal protein	PTTG_03815	2	97	Cyto	
60S acidic ribosomal protein P2	PTTG_00561	2	239	Cyto	
60S ribosomal protein	PTTG_02550	2	169	Mito	
60S ribosomal protein	PTTG_06040	2	169	Mito	
60S ribosomal protein L10A	PTTG_02133	2	443	Nucl	
60S ribosomal protein L12	PTTG_00388	2	220	Cyto	
60S ribosomal protein L13	PTTG_00212	2	189	?	
60S ribosomal protein L14	PTTG_06672	2	171	?	
60S ribosomal protein L16-A	PTTG_09845	2	169	Mito	
60S ribosomal protein L18	PTTG_03299	2	149	?	
60S ribosomal protein L18A	PTTG_00142	4	185	?	
60S ribosomal protein L19	PTTG_01400	2	220	Mito	
60S ribosomal protein L21	PTTG_01999	2	96	?	
60S ribosomal protein L23A	JF002.BU672714_TR75.T7.pth (BU672714)	2	129	?	
60S ribosomal protein L24	PTTG_07830	3	216	Nucl	
60S ribosomal protein L27E	PTTG_01168	2	93	Mito	
60S ribosomal protein L3	PTTG_05888	6	699	Mito	
60S ribosomal protein L30	PTTG_00944	2	175	Mito	
60S ribosomal protein L4	PTTG_02409	6	435	Mito	
60S ribosomal protein L6	PTTG_03532	5	245	?	

Table 2. Continued

Protein description[a)]	Protein ID[b)]	No. of peptides matching	MASCOT score	Localization[c)]	Secreted[d)]
60S ribosomal protein L7	PTTG_09820	4	287	?	
60S ribosomal protein L8	PTTG_07146	3	273	Mito	
60S ribosomal protein L9	PTTG_05820	3	99	?	
Elongation factor 1	PTTG_08852	5	140	Cyto	
Elongation factor 3	PTTG_00208	2	89	Cyto	
Elongation factor 3	PTTG_06112	6	313	Cyto	
Eukaryotic translation initiation factor 3	PTTG_02054	2	54	Nucl	
Eukaryotic translation initiation factor 3	PTTG_02526	6	182	?	Yes
Eukaryotic translation initiation factor 4A	PTTG_05192	2	79	Cysk	
Eukaryotic translation initiation factor 4A	PTTG_10185	2	79	Mito	
P-loop containing nucleoside triphosphate hydrolase	PTTG_00994	4	160	Cyto	
Ribosomal protein L15	PTTG_01482	2	117	Mito	
Ribosomal protein L15	PTTG_02501	2	117	Mito	
Ribosomal protein L5	PTTG_08056	4	211	?	
Ribosomal protein L7A	PTTG_03354	3	122	?	
Ribosomal protein S18	PTTG_07368	2	70	Nucl	
Ribosomal protein S19P	PTTG_00560	2	104	Nucl	
Ribosomal protein S2	PTTG_01758	6	625	Cyto	
Ribosomal protein S24/S35, mitochondrial	PTTG_09764	2	112	Mito	
Ribosomal protein S7	PTTG_05632	2	127	Mito	
Ribosomal protein S9	PtContig5662 (HP457009)	2	115	Mito	
Ribosomal-ubiquitin fusion protein Ubi2	PTTG_05179	2	192	Mito	
Translation elongation factor G	PGTG_12253	2	90	Mito	
Translation initiation factor 3F	PTTG_05152	3	102	Mito	
Translation initiation factor eIF-2A	PTTG_09934	3	90	?	
Small molecule transport					
Calcium-transporting ATPase	PTTG_06291	4	182	Plas	
Ferrochelatase	PTTG_01335	2	89	Mito	
Mitochondrial carrier protein related	PtContig5161 (EZ116175)	12	2270	Mito	
Mitochondrial carrier protein related	PTTG_01978	2	216	Cyto	
Mitochondrial carrier protein related	PTTG_08687	14	800	Extr	
Potassium-transporting ATPase	PTTG_02832	5	149	Plas	
Succinate/fumarate mitochondrial transporter	PTTG_02502	6	316	Cyto	
Sugar transporter	PTTG_05441	3	168	Plas	
Voltage-dependent anion-selective channel	PTTG_03877	9	1235	?	
Xenobiotics biodegradation and metabolism					
3-Ketoacyl-CoA thiolase A	PTTG_01667	2	172	Mito	
3-Oxoacyl-(acyl-carrier-protein) reductase	PTTG_02273	2	131	Cyto	
Aldo/keto reductase	PTTG_08772	3	125	Cyto	
Heme-dependent peroxidase	PTTG_01294	6	405	Mito	
Microsomal glutathione *S*-transferase 3	PTTG_05874	2	118	Mito	
Peroxiredoxin-5	PTTG_01237	2	153	?	
Unclassified proteins					
14-3-3 protein	PGTG_19162	2	192	?	
14-3-3 protein	PTTG_05801	4	128	Nucl	
Acidic mitochondrial matrix glycoprotein p32	PTTG_05417	3	134	Mito	
Differentiation-related protein Infp	PTTG_02719	4	151	Plas	Yes
Differentiation-related protein Infp	PTTG_01715	2	170	Extr	
Guanine nucleotide binding protein β subunit	PTTG_00389	5	169	?	
Hypothetical protein	PTTG_00973	5	272	Nucl	
Hypothetical protein	PtContig2570 (EZ116161) $	2	99	?	
Hypothetical protein	PtContig8071 (EZ116213)	3	200	?	

Table 2. Continued

Protein description[a)]	Protein ID[b)]	No. of peptides matching	MASCOT score	Localization[c)]	Secreted[d)]
Hypothetical protein	PtContig8194 (EZ116215)	3	247	?	
Hypothetical protein	PT03328.G08.S6Wu.ptih (GR499969)	3	56	Mito	
Hypothetical protein	PTTG_00925 $	2	57	Plas	
Hypothetical protein	PTTG_03941	2	112	Mito	
Hypothetical protein	**PTTG_06324 $**	**2**	**72**	**Extr**	**Yes**
Hypothetical protein	**PTTG_04892 $**	**4**	**549**	**Extr**	**Yes**
Hypothetical protein	**PTTG_05625**	**2**	**119**	**Extr**	**Yes**
Hypothetical protein	**PTTG_05834 $**	**2**	**152**	**Extr**	**Yes**
Hypothetical protein	**PTTG_06270 $**	**3**	**115**	**Mito**	**Yes**
Hypothetical protein	PtContig2863 (EZ116167) $	3	132	Mito	
Hypothetical protein	PTTG_04458	3	280	Extr	
Hypothetical protein	**PTTG_03653 $**	**4**	**325**	**Extr**	**Yes**
Hypothetical protein	PtContig306 (HP452079) $	4	282	Nucl	
Hypothetical protein; Uf-HSP42c stage specific secretome	PTDH.cn565.na.ptih (GR503900) $	1	69	Mito	Yes
MRS7 family protein	PTTG_09254	3	163	Nucl	
Polyadenylate-binding protein	PTTG_05898	10	561	?	
Polyprotein	PtContig7569 (EZ116198)	2	118	?	
Prichextensn	PTTG_09034	2	266	Extr	Yes
PTP1 pro-resilin gene family	PTTG_05956	3	85	?	
Septin	PTTG_03465	4	161	Nucl	
tetratricopeptide (TPR) repeat domain containing protein	PTTG_04803	4	184	?	
Tetratricopeptide repeat (TPR) containing protein	PTTG_10045	4	184	?	

a) For an extended version of this table, including peptide matches, see Supporting Information Table S1 and captions.

b) Predicted Pt protein/Pt EST/predicted Pgt protein; accession numbers can be found in the Puccinia database at http://www.broadinstitute.org/annotation/genome/puccinia_group/MultiHome.html or at NCBI http://blast.ncbi.nlm.nih.gov/Blast.cgi when in between parentheses. Proteins marked with an asterisk were also identified in the 2-D gel approach (Supporting Information Fig. S1); two proteins identified only in the 2-D gel approach are marked with ♯; proteins for which mRNA levels were analyzed by qRT-PCR (Fig. 4) are marked with $.

c) Protein localizations inferred by Wolf PSORT: ?, no reliable prediction could be inferred; Cyto, cytoplasmic; Cysk, cytoskeleton; Extr, extracellular (secreted); Mito, mitochondrial; Nucl, nuclear; Plas, plasma membrane.

d) Consensus prediction of extracellular secretion using several softwares: TargetP, SignalP and TMHMM.

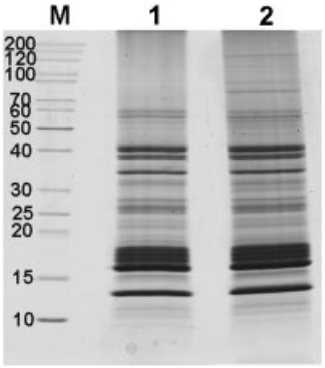

Figure 3. SDS-PAGE gel of protein samples. M: MW markers with masses indicated in kDa. Lane 1: control lane with proteins from oil-inoculated leaves, isolated using the same procedure. Lane 2: proteins from sucrose-density gradient enriched haustoria. Lane 2 was cut into ten slices, proteins digested with trypsin and analyzed by LC-MS/MS.

carried out using a combination of SignalP 3.0 [34], TargetP 1.1 [46] and TMHMM 2.0 [35], according the criteria adopted for defining the poplar leaf rust secretome [37]. SignalP results were verified against TargetP predictions to exclude proteins targeted to organelles, for example, and against TMHMM to remove proteins with transmembrane domains. This yielded 26 proteins with predicted secretory signal peptides and putatively secreted (Table 2, column 'Secreted') although five of these were not predicted by PSORT to be located extracellularly. Thirdly, although this is an indirect method, all proteins were searched against sets of potentially secreted proteins predicted using the method by Joly et al. [37] from the preliminary partial *Pt* genome and several related rust fungal genomes. These predicted 'secretome' proteins included 758 *Pt* proteins, 1699 *Pgt* proteins and 689 protein sequences derived from assembled EST sequences from various *Melampsora* poplar leaf rust fungal species (S+ category in [37]). In addition, we queried 28 identified flax rust fungus, *Melampsora lini* haustoria-specific secreted

proteins [21], 100 bean rust fungus, *U. fabae*, secretome proteins [22] and 387 predicted secreted proteins in the corn smut fungus, *Ustilago maydis* [47]. By this method, 39 *Pt* proteins in our list matched predicted *Pt* 'secretome' proteins or potentially secreted homologous proteins in other fungal species (Supporting Information Table S1). By evaluating the results of the three methods, 50 proteins were predicted secreted. Six proteins have characteristics of secreted effectors: relatively small proteins of between 100 and 300 amino acids, having a signal peptide of 15–22 amino acids at the N-terminal end, and predicted to be secreted by various programs (bold in Table 2 and Supporting Information Table S1). Among these six potential effectors, some match related paralogs that appear to constitute clusters in some cases. For example, PTTG_04892 matches four proteins in *Pt*, PTTG_01186, PTTG_04631, PTTG_00662 and PTTG_00664, the latter of which appear to belong to a cluster; there are also two homologs in *Pgt* (PGTG_09984 and PGTG_09975). Also, PTTG_05625 and PTTG_05834 are related (as can be seen from their respective protein sequences; Supporting Information Table S1) and match in various degrees of similarity 20 sequences in the *Pt* and 21 in the *Pgt* genomes; some of these also appear to be clustered.

3.7 Transcription of corresponding genes

Putative transcription profiles of the genes coding for the identified proteins were gleaned from data in our *Pt* EST database (over 40 000 ESTs deposited in GenBank). The collection of non-redundant unigenes allowed a preliminary look at tentative gene expression levels based on transcript abundance in certain stage-specific libraries: resting urediniospores ('ptu'), urediniospores germinated in vitro over water ('ptg'), dormant teliospores ('ptt'), pycniospores ('ptp'), aeciospores ('pte'), infected wheat plants ('pth') and isolated haustoria ('ptih'). The latter two stages would represent most closely the material used for the proteomics analysis presented in this study. An assessment in a previous smaller collection by semi-quantitative real-time PCR indicated that redundancy of ESTs in the generated cDNA libraries generally reflected expression levels [6]. Among the 264 proteins, 144 were identified through *Pt* EST contigs or singlets, or through *Pt* genome-predicted proteins which had representation in the *Pt* unigene database. Of the 16 that were identified among homologs in the predicted *Pgt* proteome, 9 were represented in the *Pt* EST database. Among all the matching *Pt* EST database sequences, 93 were contigs and 36 of these were composed of at least 50% of ESTs belonging to libraries representing wheat infection stages 'pth' and/or 'ptih'. For 25 proteins, we found ESTs exclusively from the isolated haustoria cDNA libraries. This suggests induced transcription during wheat infection for genes coding for some of the identified proteins.

We therefore performed quantitative real-time PCR to verify more precisely the expression of ten genes coding for proteins in our list. All ten selected genes, among which were five predicted secreted effectors (bold face in Table 2 and Supporting Information Table S2), were expressed at a significantly higher level compared with in vitro urediniospore stages, in infected compatible wheat at 123 h post-inoculation, a time when extensive fungal growth occurs with numerous haustoria present and 1–2 days before sporulation occurs (Fig. 4). Four genes seem to be expressed exclusively during plant infection, represented, for example, by PtContig306 (having four ESTs from the 'ptih' and one from the 'pth' stage), PTTG_06270 (having ESTs solely from the 'ptih' stage) and PTDH.cn565.na.ptih, thereby correlating well with the generated ESTs.

4 Discussion

In this study, we present the first proteome of haustorial infection structures from a cereal rust fungus, the leaf rust fungus *P. triticina* parasitizing wheat. This pathogen is a representative of several cereal-infecting biotrophic fungi that depend exclusively on their host for survival. Because these organisms are very refractory to molecular genetic manipulation through transformation, the generation of genomic-type resources to allow for gene/protein discovery is currently the most productive option of making inroads into understanding the infection strategies of these fungi. A recent technique allowing genetic transformation of the flax rust fungus is promising but relies on the availability of avirulence genes for selection [48]. This is currently not yet an option for cereal rust fungi.

We successfully optimized a method to obtain samples enriched for haustoria. Microscopic and molecular analyses of samples during the enrichment procedure (Figs. 1 and 2) showed that we have obtained preparations containing mostly haustorial structures with a fraction of wheat chloroplasts. We were subsequently able to produce peptide mixtures from these haustorium-enriched preparations using the GeLC-MS approach. Searches of the generated peptide spectra against the custom-made database identified over 260 fungal proteins, mostly among the *Pt* genome-predicted proteins. The fact that 16 *Pgt* proteins were identified and 20 through the *Pt* EST database most likely reflects the fact that we only have a partial proteome predicted from the currently incomplete *Pt* genome. Indeed, TBLASTN searches using *Pt* EST-predicted (partial) protein sequences as queries on all available *Pt* genomic reads resulted often in good (partial) matches indicating the presence of not yet-assembled genome sequences that have therefore failed to predict full-length open-reading frames and proteins. Several proteins identified through the peptide profiles matched haustorium-specific cDNAs in other fungal pathosystems (Table 2 and Supporting Information Table S1) and many could be matched to ESTs from isolated

haustoria-specific cDNA libraries; this further suggests that we have generated a mainly haustorial proteome.

We found several proteins predicted to be located in the membrane (ATPases, transporters, etc.) suggesting that the protein isolation method used does solubilize such proteins. We are currently uncertain as to whether the extra-haustorial matrix (ehm) co-purifies with our haustorial isolation procedure and whether proteins embedded in it can be resolved with our approach. The interface is thought to be a traffic hub for the secretion of fungal effectors and uptake of essential nutrients for the fungus [2, 12, 49]. It also has been shown to embed host proteins, including defense-related components [50]. The fact that we identified an *U. fabae* hexose transporter, HXT1 homolog which was found in abundance in the ehm [51], suggests that our method could be successful in revealing ehm-specific proteins. Future experiments are targeted at purifying and analyzing this interface more exhaustively.

The MASCOT search identified 17 proteins that, even upon extensive searches across various databases, could not be annotated with a function (Table 2 and Supporting Information Table S2). However, all were related to predicted proteins in other rust fungi (wheat stem and stripe rusts, poplar, bean and soybean rusts) such as hypothetical proteins PTTG_05625 and PTTG_05834, which matched cDNA sequences obtained from *P. striiformis*-infected wheat. Significantly, six proteins matched sequences that had been identified in the bean rust fungus as derived from haustorium-specific secretome cDNAs (Table 2 and Supporting Information Table S2). For example, one was coded for by EST PTDH.cn565.na.ptih, which matched *U. fabae* stage-specific secretome cDNA clone Uf-HSP42c, previously identified in a haustoria-specific library and predicted to contain an N-terminal signal peptide and to be secreted [20, 22]. We showed that the corresponding *Pt* gene was also exclusively expressed during plant infection (Fig. 4). In the flax rust fungus *M. lini*, several of such small

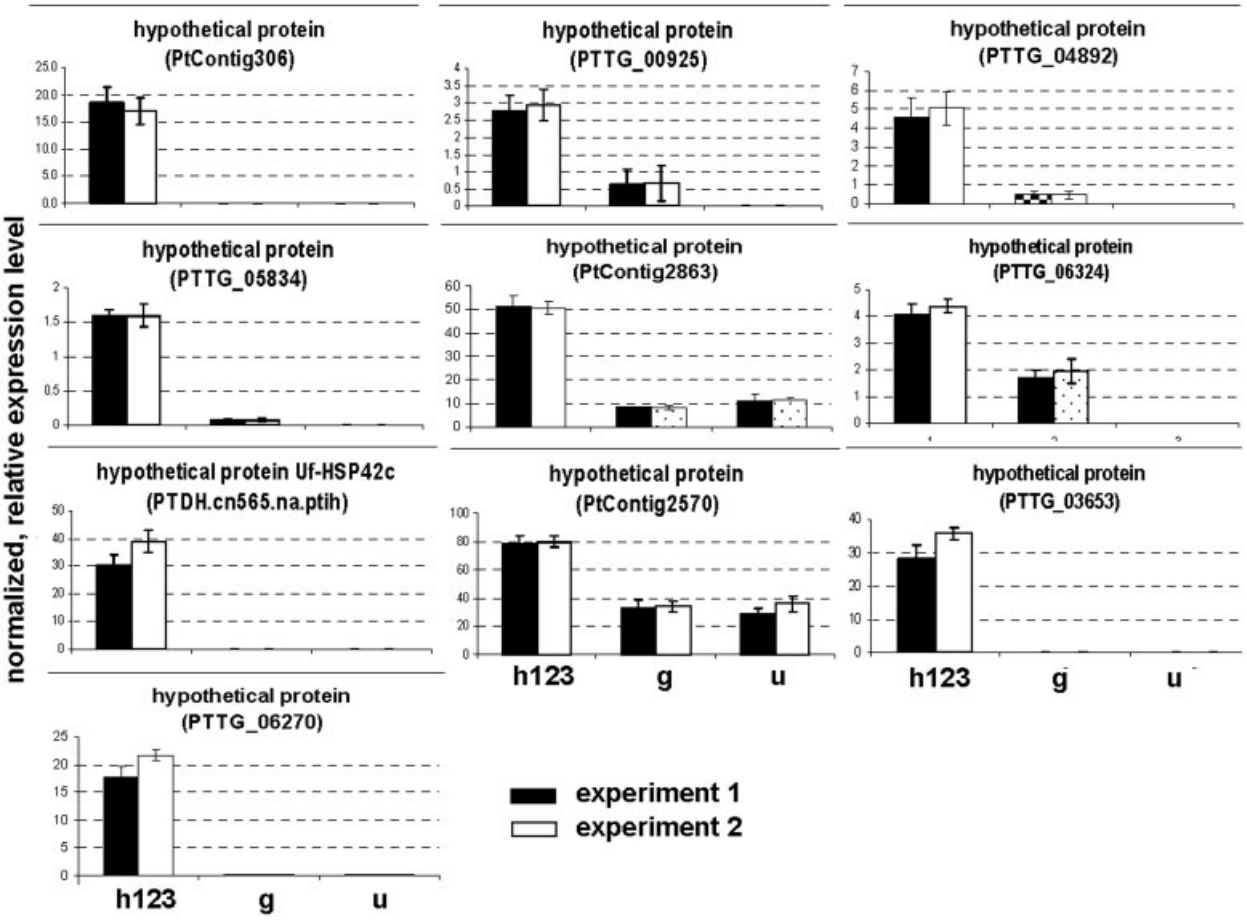

Figure 4. Expression profiles of ten genes representing selected identified proteins. Quantitative RT-PCR was performed on RNA samples from various life-cycle stages: h123h, heavily infected leaf material at haustorial stage at 123 h post-inoculation; g, urediniospores germinated in vitro over water; u, resting urediniospores. Values on the *y*-axis represent relative amounts of cDNA product in arbitrary units normalized to *Pt* α-tubulin and succinate dehydrogenase gene expression (see Section 2). Standard deviation shown is averaged over three independent biological replicate samples for each stage; in addition, two technical replicates (exp1, solid bars, and exp2, open bars) are shown for each measurement.

proteins have been shown to be secreted into the host cell with some of them displaying avirulence functions and eliciting host defense responses [21, 52]. In a recent study of the rice blast fungus *M. oryzae* biotrophic invasive hyphae (functionally analogous to rust haustoria), a large complement of predicted secreted effectors was revealed, one of which was a known avirulence factor and four of which were shown to be secreted [53]. In general, these are relatively small proteins of between 100 and 300 amino acids. This study shows that our proteomics approach can isolate and identify such characteristic factors and we are currently focusing on gel fractions containing these low molecular weight proteins.

Some of the 50 proteins predicted to be secreted have been shown in other systems to be secreted and to play crucial roles in fungal pathogenicity and interactions with host cells. Examples are: a glucan 1,3 β-glucosidase and chitinases, possibly involved in cell wall biogenesis and integrity. A peptidase and proteases, with functions that have been implicated in pathogenicity possibly by modifying host factors [54–57]. A carboxypeptidase, a mannosyl-oligosaccharide glucosidase, possibly involved in fungal cell wall protein modifications which can affect virulence such as shown for *Candida* and *Aspergillus* [58, 59]. Subtilisin-like serine proteases that likely contribute to the penetration of the plant cuticle and cell wall [60, 61]. Protein disulfide isomerases catalyze transitions of disulfide bonds, whose formations play important roles in folding and stabilizing of proteins secreted to the extracellular medium, especially those acting in the plant apoplast [62, 63]. Cyclophilins, of which we have identified three with two predicted secreted, have been reported as important virulence factors. This has been demonstrated, for example, in the infection of rice by the ascomycete fungus *Magnaporthe grisea* [64], in the facultative human pathogenic yeast *Cryptococcus neoformans* [65], and in the later infection stages of plant colonization by *Botrytis cinerea* [66]. An identified trehalose-phosphatase catalyzes the last biosynthesis step in the production of trehalose, a sugar that has been shown to be critical for cell wall integrity and virulence in many human and plant fungal pathogens [67–70]. Interestingly, trehalose phosphatase is involved in trehalose synthesis which takes place in the cytoplasm. However, it is suggested to be secreted by *Pt* in our study as well as by the flax rust fungus [21]. These results may imply another function of this protein. Another predicted secreted protein that may function in virulence is a possible sugar transporter homolog which was found in abundance in the extra-haustorial matrix of bean rust haustoria [51].

Of great interest are proteins involved in pathogenicity, virulence and fungal self-defense, i.e. cell rescue. These will likely include the above-mentioned effectors but might also include the mentioned chitinase and superoxide dismutase. The latter protein has been shown to be involved in the stress response of organisms encountering an oxidative host environment triggered upon their invasion when its expression is induced, for example, in *U. fabae* infecting bean leaves [20] and during *C. neoformans* infection [71]. The identified superoxide dismutase gene, represented by PTTG_05861, seemed to be expressed in all three stages though to a threefold higher level during infection (data not shown). Significant might be the sizable production of HSPs (Table 2 and Supporting Information Table S1). In cells, a chaperone protein network functions in both initial protein folding and subsequent maintenance of proteins. Conventionally, elevated levels of HSPs were found upon heat stress to protect proteins and maintain correct folding, but recent literature indicates roles in preventing protein aggregation, controlling protein turn-over, increasing life span and virulence [72]. For example, overexpression of a HSP90 in *Saccharomyces cerevisiae* (HSP82 homolog) increased its weak virulence in mice [73]. In *Candida albicans*, HSP70 was found on the cell surface and it was hypothesized that this chaperone could act as a 'smoke screen' preventing an effective host immune response [74]. Interestingly, two proteins in the chaperone class we identified have predicted secretion signals and are predicted to be located extra-cellularly. Elevated expression of HSP genes was also found during *C. neoformans* infection [71]. The multiple HSPs found in *Pt* haustoria could serve similar roles and/or indicate a reaction to elevated stress while the fungus is battling host defense responses and needs to protect vital components, as was hypothesized in [24]. In that study, elevated levels of many identified HSPs/chaperons were found in haustoria from the barley powdery mildew fungus, *B. graminis*, compared with urediniospores. However, a large complement of HSPs was also discovered in urediniospores of the bean rust fungus, *U. appendiculatus* [75]. Such spores differentiate from hyphae roaming through infected host tissue and are connected to myriad haustoria. A more precise analysis of levels of expression of the various HSPs in different *P. triticina* life-cycle stages is needed to obtain information about their possible roles.

Our study reveals an extensive set of ribosomal structural proteins and proteins involved in energy conversion and general metabolism. This is consistent with the presumed function of the haustorium as a nutrient sink from the plant perspective and a feeding structure for the developing fungus. Whether this reflects an increase in the production of these proteins in infection structures compared with urediniospore stages, e.g. during germination and pre-infection, cannot be assessed here since no comparative proteomic analysis of such fungal stages was performed. However, from our previous analysis of an initial 25 000 *Pt* ESTs, higher normalized EST counts were identified for such energy-related genes (e.g. cytochrome *c* complex) and ribosomal proteins recovered from wheat infection stages compared with dormant urediniospores and in vitro germinated urediniospores [6]. Similarly, higher numbers of tags were obtained from samples from infection stages than from urediniospore stages for ubiquitin, actin (mitochondrial) ATPase and ATP synthase complex units and several proteins possibly involved in virulence and defense such as chitinase, superoxide dismutase and several HSPs. In other studies of the *P. triti-*

cina wheat-infection stage, increased protein synthesis and metabolism was also inferred from ESTs with homology to ribosomal proteins and metabolic and energy-related enzymes [76, 77]. EST inventories representing infection stages in other pathosystems have also suggested increased ribosomal activities and metabolism such as described for the wheat stem rust fungus *P. graminis* [78] and the wheat leaf blotch ascomycete fungus, *Mycosphaerella graminicola* [79, 80]. Analyses on cDNA microarrays also indicated increased expression of genes involved in glycolysis (energy) and protein biosynthesis during the interaction of the biotrophic ascomycete fungus *B. graminis* infecting barley [81, 82]. In the latter fungus, a partial proteome of haustoria also revealed relatively high representation of proteins involved in protein metabolic pathways and energy production [23], and a comparative proteomic analysis substantiated increased production of proteins involved in protein and energy metabolism in haustoria [24].

Previously, we generated protein profiles of the wheat host during a susceptible interaction with *P. triticina* [30]. The current data set is a first successful glimpse at a partial protein complement in a crucial cereal rust fungal pathogen infection structure. Our current efforts are geared towards analyzing more in depth haustorial membrane and extra-haustorial matrix fractions and generating proteomes from other life-cycle stages for comparative analyses. With the anticipated complete genome-derived comprehensive predicted protein inventory, future analyses will undoubtedly reveal additional proteins with major functions in pathogenicity, virulence and vital developmental stages. The targeting of such 'Achilles heels' in this pathogen is an overarching goal to combat this disease in cereal crops.

The authors are very much indebted to James Chong for supplying the TEM pictures of haustoria and to Pat Seto-Goh and Jacqueline Ching for excellent technical assistance. The authors also greatly acknowledge the funding from NSF/USDA grant 2008-35600-04693 to support the work done at the Broad Institute, Cambridge, MA, in generating the initial P. triticina genome reads (C. Cuomo, L. Szabo, J. Fellers and G. Bakkeren). The authors thank greatly John Fellers and Matthew Dickinson for contributing a cDNA library and EST sequences to the database. Part of the EST sequencing was funded through a collaborative grant from the Natural Sciences and Engineering Research Council of Canada Strategic Project to Barry Saville and G.B. The proteomics research was funded by the Agriculture and Agri-Food Canada' Canadian Crop Genomics Initiative'.

The authors have declared no conflict of interest.

5 References

[1] Altschul, S. F., Gish, W., Miller, W., Myers, E. W., Lipman, D. J., Basic local alignment search tool. *J. Mol. Biol.* 1990, *215*, 403–410.

[2] Hogenhout, S. A., Van der Hoorn, R. A., Terauchi, R., Kamoun, S., Emerging concepts in effector biology of plant-associated organisms. *Mol. Plant Microbe Interact.* 2009, *22*, 115–122.

[3] Leonard, K. J., Szabo, L. J., Stem rust of small grains and grasses caused by *Puccinia graminis*. *Mol. Plant Pathol.* 2005, *6*, 99–111.

[4] Bolton, M. D., Kolmer, J. A., Garvin, D. F., Wheat leaf rust caused by *Puccinia triticina*. *Mol. Plant Pathol.* 2008, *9*, 563–575.

[5] Chen, X. M., Epidemiology and control of stripe rust *Puccinia striiformis* f. sp. *tritici* on wheat. *Can. J. Plant Pathol.* 2005, *27*, 314–337.

[6] Hu, G., Linning, R. O. B., McCallum, B., Banks, T. et al., Generation of a wheat leaf rust, *Puccinia triticina*, EST database from stage-specific cDNA libraries. *Mol. Plant Pathol.* 2007, *8*, 451–467.

[7] Samborski, D. J., in: Roelfs, A. P., Bushnell, W. R. (Eds.), *The Cereal Rusts, Vol. II: Diseases, Distribution, Epidemiology and Control*, Academic Press, Orlando, FL 1985, pp. 39–59.

[8] Horton, J. S., Bakkeren, G., Klosterman, S. J., Garcia-Pedrajas, M., Gold, S. E., in: Arora, D. K., Berka, R. (Eds.), *Applied Mycology and Biotechnology. Genes and Genomics*, Elsevier, Dordrecht 2005, pp. 353–422.

[9] Chong, J., Harder, D. E., Rohringer, R., Cytochemical studies on *Puccinia graminis* f. sp. *tritici* in a compatible wheat host. II. Haustorium mother cell walls at the host cell penetration site, haustorial walls, and the extrahaustorial matrix. *Can. J. Bot.* 1986, *64*, 2561–2575.

[10] Samborski, D. J., Dyck, P. L., Inheritance of virulence in wheat leaf rust on the standard differential wheat varieties. *Can. J. Genet. Cytol.* 1968, *10*, 24–32.

[11] Mendgen, K., Struck, C., Voegele, R. T., Hahn, M., Biotrophy and rust haustoria. *Physiol. Mol. Plant Pathol.* 2000, *56*, 141–145.

[12] Voegele, R. T., Mendgen, K., Rust haustoria: nutrient uptake and beyond. *New Phytol.* 2003, *159*, 93–100.

[13] Ellis, J. G., Dodds, P. N., Lawrence, G. J., The role of secreted proteins in diseases of plants caused by rust, powdery mildew and smut fungi. *Curr. Opin. Microbiol.* 2007, *10*, 326–331.

[14] Mudgett, M. B., New insights to the function of phytopathogenic bacterial type III effectors in plants. *Annu. Rev. Plant Biol.* 2005, *56*, 509–531.

[15] Mueller, C. A., Broz, P., Cornelis, G. R., The type III secretion system tip complex and translocon. *Mol. Microbiol.* 2008, *68*, 1085–1095.

[16] Ellis, J., Catanzariti, A. M., Dodds, P., The problem of how fungal and oomycete avirulence proteins enter plant cells. *Trends Plant Sci.* 2006, *11*, 61–63.

[17] Dodds, P. N., Rafiqi, M., Gan, P. H. P., Hardham, A. R. et al., Effectors of biotrophic fungi and oomycetes: pathogenicity factors and triggers of host resistance. *New Phytol.* 2009, *183*, 993–1000.

[18] Niks, R. E., Comparative histology of partial resistance and the nonhost reaction to leaf rust pathogens in barley and wheat seedlings. *Phytopathology* 1983, *73*, 60–64.

[19] Hu, G., Rijkenberg, F. H. J., Scanning electron microscopy of early infection structure formation by *Puccinia recondita* f. sp. *tritici* on and in susceptible and resistant wheat lines. *Mycol. Res.* 1998, *102*, 391–399.

[20] Jakupovic, M., Heintz, M., Reichmann, P., Mendgen, K., Hahn, M., Microarray analysis of expressed sequence tags from haustoria of the rust fungus *Uromyces fabae*. *Fungal Genet. Biol.* 2006, *43*, 8–19.

[21] Catanzariti, A. M., Dodds, P. N., Lawrence, G. J., Ayliffe, M. A., Ellis, J. G., Haustorially expressed secreted proteins from flax rust are highly enriched for avirulence elicitors. *Plant Cell* 2006, *18*, 243–256.

[22] Link, T. I., Voegele, R. T., Secreted proteins of *Uromyces fabae*: similarities and stage specificity. *Mol. Plant Pathol.* 2008, *9*, 59–66.

[23] Godfrey, D., Zhang, Z., Saalbach, G., Thordal-Christensen, H., A proteomics study of barley powdery mildew haustoria. *Proteomics* 2009, *9*, 3222–3232.

[24] Bindschedler, L. V., Burgis, T. A., Mills, D. J., Ho, J. T. et al., In planta proteomics and proteogenomics of the biotrophic barley fungal pathogen *Blumeria graminis* f. sp. *hordei*. *Mol. Cell. Proteomics* 2009, *8*, 2368–2381.

[25] de Godoy, L. M., Olsen, J. V., de Souza, G. A., Li, G. et al., Status of complete proteome analysis by mass spectrometry: SILAC labeled yeast as a model system. *Genome Biol.* 2006, *7*, R50.

[26] Long, D. L., Kolmer, J. A., A North American system of nomenclature for *Puccinia recondita* f. sp. *tritici*. *Phytopathology* 1989, *79*, 525–529.

[27] Tiburzy, R., Martins, E. M. F., Reisener, H. J., Isolation of haustoria of *Puccinia graminis* f. sp. *tritici* from wheat leaves. *Exp. Mycol.* 1992, *16*, 324–328.

[28] Rohringer, R., Kim, W., Samborski, D. J., Howes, N. K., Calcofluor: an optical brightner for fluorescence microscopy of fungal plant parasites. *Phytopathology* 1976, *67*, 808–810.

[29] Berruyer, R., Poussier, S., Kankanala, P., Mosquera, G., Valent, B., Quantitative and qualitative influence of inoculation methods on in planta growth of rice blast fungus. *Phytopathology* 2006, *96*, 346–355.

[30] Rampitsch, C., Bykova, N. V., McCallum, B., Beimcik, E., Ens, W., Analysis of the wheat and *Puccinia triticina* (leaf rust) proteomes during a susceptible host–pathogen interaction. *Proteomics* 2006, *6*, 1897–1907.

[31] Rampitsch, C., Bykova, N. V., Methods for functional proteomic analyses. *Methods Mol. Biol.* 2009, *513*, 93–110.

[32] Perkins, D. N., Pappin, D. J., Creasy, D. M., Cottrell, J. S., Probability-based protein identification by searching sequence databases using mass spectrometry data. *Electrophoresis* 1999, *20*, 3551–3567.

[33] Nielsen, H., Engelbrecht, J., Brunak, S., von Heijne, G., Identification of prokaryotic and eukaryotic signal peptides and prediction of their cleavage sites. *Protein Eng.* 1997, *10*, 1–6.

[34] Dyrløv Bendtsen, J., Nielsen, H., von Heijne, G., Brunak, S., Improved prediction of signal peptides: SignalP 3.0. *J. Mol. Biol.* 2004, *340*, 783–795.

[35] Krogh, A., Larsson, B., von Heijne, G., Sonnhammer, E. L., Predicting transmembrane protein topology with a hidden Markov model: application to complete genomes. *J. Mol. Biol.* 2001, *305*, 567–580.

[36] Horton, P., Park, K. J., Obayashi, T., Fujita, N. et al., WoLF PSORT: protein localization predictor. *Nucleic Acids Res.* 2007, *35*, W585–W587.

[37] Joly, D., Feau, N., Tanguay, P., Hamelin, R., Comparative analysis of secreted protein evolution using expressed sequence tags from four poplar leaf rusts (*Melampsora* spp.). *BMC Genomics* 2010, *11*, 422.

[38] Harder, D. E., Chong, J., in: Bushnell, W. R., Roelfs, A. P. (Eds.), *The Cerreal Rusts. Vol. I. Origins, Specificity, Structure and Physiology*, Academic Press, Orlando, FL 1984, pp. 333–373.

[39] Hu, G. G., Rijkenberg, F. H. J., Ultrastructural studies of the intercellular hypha and haustorium of *Puccinia recondita* f. sp. *tritici*. *J. Phytopathol.* 1998, *146*, 39–50.

[40] Hahn, M., Mendgen, K., Isolation of ConA binding of haustoria from different rust fungi and comparison of their surface qualities. *Protoplasma* 1992, *170*, 95–103.

[41] Hahn, M., Mendgen, K., Characterization of in planta-induced rust genes isolated from a haustorium-specific cDNA library. *Mol. Plant Microbe Interact.* 1997, *10*, 427–437.

[42] Kemen, E., Kemen, A. C., Rafiqi, M., Hempel, U. et al., Identification of a protein from rust fungi transferred from haustoria into infected plant cells. *Mol. Plant Microbe Interact.* 2005, *18*, 1130–1139.

[43] Cooper, B., Neelam, A., Campbell, K. B., Lee, J. et al., Protein accumulation in the germinating *Uromyces appendiculatus* uredospore. *Mol. Plant Microbe Interact.* 2007, *20*, 857–866.

[44] Puthoff, D. P., Neelam, A., Ehrenfried, M. L., Scheffler, B. E. et al., Analysis of expressed sequence tags from *Uromyces appendiculatus* hyphae and haustoria and their comparison to sequences from other rust fungi. *Phytopathology* 2008, *98*, 1126–1135.

[45] Kanehisa, M., Goto, S., Kawashima, S., Okuno, Y., Hattori, M., The KEGG resource for deciphering the genome. *Nucleic Acids Res.* 2004, *32*, D277–D280.

[46] Emanuelsson, O., Brunak, S., von Heijne, G., Nielsen, H., Locating proteins in the cell using TargetP, SignalP and related tools. *Nat. Protoc.* 2007, *2*, 953–971.

[47] Mueller, O., Kahmann, R., Aguilar, G., Trejo-Aguilar, B. et al., The secretome of the maize pathogen *Ustilago maydis*. *Fungal Genet. Biol.* 2008, *45*, S63–S70.

[48] Lawrence, G. J., Dodds, P. N., Ellis, J. G., Transformation of the flax rust fungus, *Melampsora lini*: selection via silencing of an avirulence gene. *Plant J.* 2010, *61*, 364–369.

[49] Micali, C. O., Neumann, U., Grunewald, D., Panstruga, R., O'Connell, R., Biogenesis of a specialized plant–fungal interface during host cell internalization of *Golovinomyces orontii* haustoria. *Cell Microbiol.* doi: 10.1111/J.1462-5822.2010.01530.x.

[50] Wang, W., Wen, Y., Berkey, R., Xiao, S., Specific targeting of the *Arabidopsis* resistance protein RPW8. 2 to the interfacial

membrane encasing the fungal haustorium renders broad-spectrum resistance to powdery mildew. *Plant Cell* 2009, *21*, 2898–2913.

[51] Voegele, R. T., Struck, C., Hahn, M., Mendgen, K., The role of haustoria in sugar supply during infection of broad bean by the rust fungus *Uromyces fabae*. *Proc. Natl. Acad. Sci. USA* 2001, *98*, 8133–8138.

[52] Dodds, P. N., Lawrence, G. J., Catanzariti, A. M., Teh, T. et al., Direct protein interaction underlies gene-for-gene specificity and coevolution of the flax resistance genes and flax rust avirulence genes. *Proc. Natl. Acad. Sci. USA* 2006, *103*, 8888–8893.

[53] Mosquera, G., Giraldo, M. C., Khang, C. H., Coughlan, S., Valent, B., Interaction transcriptome analysis identifies *Magnaporthe oryzae* BAS1-4 as biotrophy-associated secreted proteins in rice blast disease. *Plant Cell* 2009, *21*, 1273–1290.

[54] Jia, Y., McAdams, S. A., Bryan, G. T., Hershey, H. P., Valent, B., Direct interaction of resistance gene and avirulence gene products confers rice blast resistance. *EMBO J.* 2000, *19*, 4004–4014.

[55] Roden, J., Eardley, L., Hotson, A., Cao, Y., Mudgett, M. B., Characterization of the *Xanthomonas* AvrXv4 effector, a SUMO protease translocated into plant cells. *Mol. Plant Microbe Interact.* 2004, *17*, 633–643.

[56] Xia, Y., Proteases in pathogenesis and plant defence. *Cell Microbiol.* 2004, *6*, 905–913.

[57] Kim, H. S., Desveaux, D., Singer, A. U., Patel, P. et al., The *Pseudomonas syringae* effector AvrRpt2 cleaves its C-terminally acylated target, RIN4, from *Arabidopsis* membranes to block RPM1 activation. *Proc. Natl. Acad. Sci. USA* 2005, *102*, 6496–6501.

[58] Bates, S., de la Rosa, J. M., MacCallum, D. M., Brown, A. J. et al., *Candida albicans* Iff11, a secreted protein required for cell wall structure and virulence. *Infect. Immun.* 2007, *75*, 2922–2928.

[59] Schmalhorst, P. S., Krappmann, S., Vervecken, W., Rohde, M. et al., Contribution of galactofuranose to the virulence of the opportunistic pathogen *Aspergillus fumigatus*. *Euk. Cell* 2008, *7*, 1268–1277.

[60] Oh, Y. Y., Donofrio, N., Pan, H., Coughlan, S. et al., Transcriptome analysis reveals new insight into appressorium formation and function in the rice blast fungus *Magnaporthe oryzae*. *Genome Biol.* 2008, *9*, R85.

[61] Soanes, D. M., Alam, I., Cornell, M., Wong, H. M. et al., Comparative genome analysis of filamentous fungi reveals gene family expansions associated with fungal pathogenesis. *PLoS ONE* 2008, *3*, e2300.

[62] Kamoun, S., A catalogue of the effector secretome of plant pathogenic oomycetes. *Annu. Rev. Phytopathol.* 2006, *44*, 41–60.

[63] Rep, M., Small proteins of plant-pathogenic fungi secreted during host colonization. *FEMS Microbiol. Lett.* 2005, *253*, 19–27.

[64] Viaud, M. C., Balhadere, P. V., Talbot, N. J., A *Magnaporthe grisea* cyclophilin acts as a virulence determinant during plant infection. *Plant Cell* 2002, *14*, 917–930.

[65] Wang, P., Cardenas, M. E., Cox, G. M., Perfect, J. R., Heitman, J., Two cyclophilin A homologs with shared and distinct functions important for growth and virulence of *Cryptococcus neoformans*. *EMBO Rep.* 2001, *2*, 511–518.

[66] Viaud, M., Brunet-Simon, A., Brygoo, Y., Pradier, J. M., Levis, C., Cyclophilin A and calcineurin functions investigated by gene inactivation, cyclosporin A inhibition and cDNA arrays approaches in the phytopathogenic fungus *Botrytis cinerea*. *Mol. Microbiol.* 2003, *50*, 1451–1465.

[67] Foster, A. J., Jenkinson, J. M., Talbot, N. J., Trehalose synthesis and metabolism are required at different stages of plant infection by *Magnaporthe grisea*. *EMBO J.* 2003, *22*, 225–235.

[68] Lowe, R. G. T., Lord, M., Rybak, K., Trengove, R. D. et al., Trehalose biosynthesis is involved in sporulation of *Stagonospora nodorum*. *Fungal Genet. Biol.* 2009, *46*, 381–389.

[69] Ngamskulrungroj, P., Himmelreich, U., Breger, J. A., Wilson, C. et al., The trehalose synthesis pathway is an integral part of the virulence composite for *Cryptococcus gattii*. *Infect. Immun.* 2009, *77*, 4584–4596.

[70] Al-Bader, N., Vanier, G., Liu, H., Gravelat, F. N. et al., Role of trehalose biosynthesis in *Aspergillus fumigatus* development, stress response, and virulence. *Infect. Immun.* 2010, *78*, 3007–3018.

[71] Steen, B. R., Zuyderduyn, S., Toffaletti, D. L., Marra, M. et al., *Cryptococcus neoformans* gene expression during experimental cryptococcal meningitis. *Euk. Cell* 2003, *2*, 1336–1349.

[72] Burnie, J. P., Carter, T. L., Hodgetts, S. J., Matthews, R. C., Fungal heat-shock proteins in human disease. *FEMS Microbiol. Rev.* 2006, *30*, 53–88.

[73] Hodgetts, S., Matthews, R., Morrissey, G., Mitsutake, K. et al., Over-expression of *Saccharomyces cerevisiae* hsp90 enhances the virulence of this yeast in mice. *FEMS Immunol. Med. Microbiol.* 1996, *16*, 229–234.

[74] Eroles, P., Sentandreu, M., Elorza, M. V., Sentandreu, R., The highly immunogenic enolase and Hsp70p are adventitious *Candida albicans* cell wall proteins. *Microbiology* 1997, *143*, 313–320.

[75] Cooper, B., Garrett, W. M., Campbell, K. B., Shotgun identification of proteins from uredospores of the bean rust *Uromyces appendiculatus*. *Proteomics* 2006, *6*, 2477–2484.

[76] Thara, V. K., Fellers, J. P., Zhou, J. M., In planta induced genes of *Puccinia triticina*. *Mol. Plant Pathol.* 2003, *4*, 51–56.

[77] Zhang, L., Meakin, H., Dickinson, M., Isolation of genes expressed during compatible interactions between leaf rust (*Puccinia triticina*) and wheat using cDNA-AFLP. *Mol. Plant Pathol.* 2003, *4*, 469–477.

[78] Broeker, K., Bernard, F., Moerschbacher, B. M., An EST library from *Puccinia graminis* f. sp. *tritici* reveals genes potentially involved in fungal differentiation. *FEMS Microbiol. Lett.* 2006, *256*, 273–281.

[79] Keon, J., Antoniw, J., Rudd, J., Skinner, W. et al., Analysis of expressed sequence tags from the wheat leaf blotch

pathogen *Mycosphaerella graminicola* (anamorph *Septoria tritici*). *Fungal Genet. Biol.* 2005, *42*, 376–389.

[80] Kema, G. H. J., van der Lee, T. A. J., Mendes, O., Verstappen, E. C. P. et al., Large-scale gene discovery in the *Septoria tritici* blotch fungus *Mycosphaerella graminicola* with a focus on *in planta* expression. *Mol. Plant Microbe Interact.* 2008, *21*, 1249–1260.

[81] Both, M., Csukai, M., Stumpf, M. P., Spanu, P. D., Gene expression profiles of *Blumeria graminis* indicate dynamic changes to primary metabolism during development of an obligate biotrophic pathogen. *Plant Cell* 2005, *17*, 2107–2122.

[82] Both, M., Eckert, S. E., Csukai, M., Muller, E. et al., Transcript profiles of *Blumeria graminis* development during infection reveal a cluster of genes that are potential virulence determinants. *Mol. Plant Microbe Interact.* 2005, *18*, 125–133.

[83] Littlefield, L. J., Heath, M. C., *Ultrastructure of Rust Fungi*, Academic Press, New York 1979.

